36th AIAA Thermophysics Conference
23-26 June 2003, Orlando, Florida

AIAA 2003-3644

Hybrid DSMC-CFD Simulations of Hypersonic Flow Over Sharp and Blunted Bodies

Wen-Lan Wang* and Iain D. Boyd†
Department of Aerospace Engineering
University of Michigan, Ann Arbor, MI 48109

Abstract

A hybrid particle-continuum computational framework is developed and presented for simulating hypersonic interacting flows, aimed to be faster and more accurate than conventional numerical methods. The framework consists of the direct simulation Monte Carlo-Information Preservation (DSMC-IP) method coupled with a Navier-Stokes solver. Since the DSMC-IP method provides the macroscopic information in each time step, determination of the continuum fluxes across the interface between the particle and continuum domains becomes straightforward. Numerical experiments of hypersonic flows over a simple blunted cone and a much more complex hollow cylinder-flare are conducted. The solutions for the two geometries considered from the hybrid framework are compared in detail with pure particle calculations. It is concluded that the hybrid method basically works very well. Numerical accuracy improvement is achieved in simple flows but unclear in complex flows. It is also concluded that the numerical efficiency obtained with the hybrid method is far from satisfactory. Overall, the hybrid framework provides a foundation for future development.

Introduction

The flow around a space vehicle during its atmospheric re-entry always spans a very wide range of flow regimes, from the continuum to the transition, depending upon the flight altitude and the characteristic length scale of the fuselage. For many years, efforts have been undertaken on developing a particle-continuum coupled numerical method that is fast and at the same time physically accurate. Among many particle-based schemes, the direct simulation Monte Carlo (DSMC) method[1] is the most common one. The DSMC method emulates the nonlinear Boltzmann equation by simulating the real molecule collisions with collision frequencies and scattering velocity distributions determined from the kinetic theory of a dilute gas. On the other hand, among many continuum schemes, the computational fluid dynamics (CFD) method that solves the Navier-Stokes (NS) equations can be regarded as the most popular approach for these flows.

A major issue in making a combination of the two numerical methods comes from the information exchange at the interface between the particle and continuum domains. At the interface, macroscopic flow properties have to be provided to the CFD method to evaluate the net fluxes and to the DSMC method to initialize the particles entering from the continuum domain into the particle domain. Several attempts have been considered, such as the Marshak condition,[2] the kinetic flux-vector splitting (KFVS) scheme,[3,4] and adaptive mesh and algorithm refinement (AMAR) embedding a particle method.[5] To date, a robust, multi-dimensional scheme that is capable of handling nonequilibrium, hypersonic compressed flows has not yet been accomplished.

Since the DSMC technique inherits very strong statistical fluctuations, it always needs several steps of sampling before smooth macroscopic flow properties can be obtained. A hybrid approach in this fashion is considered as weakly coupled[2,6] and is inadequate for complex nonequilibrium flows. To overcome the fluctuations, Fan and Shen[7] first proposed an Information Preservation (IP) technique. The technique was later further developed by others for low speed rarefied gas flows,[8–10] such as micro-electro-mechanical systems (MEMS). In the latest development by Sun and Boyd,[11] an additional temperature term is introduced in the energy model to balance the translational energy carried by a particle moving from cell to cell.

Another issue regarding the development of a hybrid method is to know when to switch between the methods. Since it is well known that the NS equations are not valid under rarefied conditions, it is general to use a continuum breakdown parameter as the switching criterion. For the hypersonic flows mentioned above, this issue has been investigated in our previous work[12] and it is concluded that a proposed parameter

$$\mathrm{Kn}_{\max} \equiv \max\left(\mathrm{Kn}_D, \mathrm{Kn}_T, \mathrm{Kn}_V\right) \qquad (1)$$

with a threshold value of 0.05 can best predict the regions where the Navier-Stokes equations fail. The

*Graduate Student Research Assistant, AIAA Student Member, E-mail: (aerowwl@engin.umich.edu)
†Professor, AIAA Associate Fellow, E-mail: (iainboyd@engin.umich.edu)

Knudsen number in Eq. 1 is expressed as

$$\mathrm{Kn}_Q = \frac{\lambda}{Q}\left|\nabla Q\right|,$$

where Q can be any flow property in general. Since continuum breakdown is often related to the transport phenomena of viscosity and heat transfer, we only consider the flow properties of density(D), temperature(T) and magnitude of velocity(V).

In the authors' prior work,[13] a preliminary hybrid approach employing the IP method with the extra temperature term mentioned above was established and a numerical experiment of a Mach 4 supersonic flow over a 2-D wedge was conducted. The hybrid method has been further developed since for hypersonic, axi-symmetric flows. The present study is considered as an extension of the prior work. To make this paper complete and self-contained, however, the main methodology from Ref. 13 is repeated.

In the next section, a brief description of the continuum approach will be presented, followed by an introduction of the DSMC-IP method. A detailed explanation on how to combine these two methods together is provided in the section of Domain Coupling. After that, hypersonic flows over a simple blunted cone and a complex hollow cylinder-flare are considered. Detailed comparisons are made for the results from the hybrid and pure particle calculations. Summary and conclusions are provided in the last section, followed by some thoughts for further development.

Numerical Schemes

Continuum Approach

The Navier-Stokes equations in the continuum domain are solved numerically using an explicit Gauss-Seidel line relaxation method and second-order accurate, modified Steger-Warming flux vector splitting.[14] The viscosity μ is modeled with the power law

$$\mu = \mu_{\mathrm{ref}}(T/T_{\mathrm{ref}})^{\omega}$$

and the thermal conductivity κ is determined from the Prandtl number

$$\mathrm{Pr} = c_p\mu/\kappa$$

where c_p is the specific heat at constant pressure. A slip-boundary model proposed by Gökçen[15] is incorporated:

$$\vec{u}_s = \frac{2-\sigma_v}{\sigma_v}\lambda_v\frac{\partial\vec{u}}{\partial n}\Big|_w, \tag{2}$$

$$T_s = T_w + \frac{2-\sigma_T}{\sigma_T}\lambda_T\frac{\partial T}{\partial n}\Big|_w, \tag{3}$$

where T_w is the temperature of the surface, and σ_v and σ_T are the tangential momentum and thermal accommodation coefficients of the surface. Here the mean free path for momentum, λ_v, and thermal energy, λ_T are defined as

$$\lambda_v = \frac{2\mu}{\rho\bar{c}}, \qquad \lambda_T = \frac{2\kappa}{\rho\bar{c}c_v}$$

where $\bar{c} = \sqrt{8RT/\pi}$ is the mean molecular speed, and c_v is the specific heat at constant volume.

DSMC-IP Approach

The information preservation method was first developed by Fan and Shen[7] to overcome the statistical scatter problem in DSMC simulations, especially for systems in which the flow speed is much smaller than the molecular speed. In addition to the ordinary thermal velocity that is utilized to compute the particle trajectory, each simulation particle in the DSMC-IP method also possesses macroscopic preserved information such as velocity vector and temperature. As a result, the DSMC-IP method uses at most 57% more memory than in the standard DSMC method.[16] This method has achieved great success for solving microscale gas flows (see Refs. 9, 10, 17).

In each time step of the DSMC-IP method, simulation particles are first moved and collided in the usual way as in the standard DSMC method. The preserved velocity in the r_i direction and temperature of simulation particles are updated by solving

$$\frac{\partial V_i}{\partial t} = -\frac{1}{\rho_c}\frac{\partial p_c}{\partial r_i} \tag{4}$$

$$\frac{\partial}{\partial t}\left(\frac{V_i^2}{2} + \frac{\zeta\cdot R\cdot T}{2}\right) = -\frac{1}{\rho_c}\frac{\partial}{\partial r_i}\left(V_{i,c}\cdot p_c\right) \tag{5}$$

where p is the pressure, ρ is the mass density, ζ is the number of internal degrees of freedom of molecules, and the subscript c denotes the macroscopic information for the computational cells. After the preserved information of simulation particles is updated, the preserved information for cells is updated by taking the arithmetic average over the information of all N_p particles in the cell,

$$V_{i,c} = \frac{1}{N_p}\sum_{j=1}^{N_p} V_{i,j} \tag{6}$$

$$T_c = \frac{1}{N_p}\sum_{j=1}^{N_p}\left(T_j + T_{a,j}\right). \tag{7}$$

The density is updated by solving the continuity equation

$$\frac{\partial\rho_c}{\partial t} = -\frac{\partial}{\partial r_i}\left(\rho_c\cdot V_{i,c}\right). \tag{8}$$

The ideal gas law, $p = \rho RT$, is assumed. The reason for the additional temperature term, T_a, in Eq. 7 and a detailed description and implementation of the DSMC-IP method can be found in Ref. 11.

Note that an adequate numerical scheme must be employed to solve Eq. 8 due to the presence of shock

waves in supersonic flows. Since the same equation also appears in the NS equations, we use the same technique described in the last subsection.

The current DSMC-IP code is based on a parallel optimized DSMC code named MONACO.[18] A sub-cell scheme is implemented for selection of collision pairs where the number of sub-cells is scaled by the local mean free path.

Domain Coupling

To implement the coupling between the particle method and the NS solver, buffer and reservoir DSMC-IP cells are introduced in the continuum domain adjacent to the domain interface, as depicted in Fig. 1. A similar concept of reservoir cells was first proposed in Ref. 6.

The buffer DSMC-IP cells work as an extension of the particle domain. Simulation particles that end their movement phase within the pure particle domain or in the buffer cells are retained. Those that leave these two regions are removed. For each time step, all simulation particles in the reservoir cells are first deleted and then re-generated based on the cell-centered values. The number of new particles is evaluated from the cell density value and the particle velocities and temperature are initialized to the Chapman-Enskog distribution[19] based on the corresponding cell values. The newly generated particles are randomly distributed within the reservoir cells. In this study, three layers of buffer cells and two layers of reservoir cells are employed.

In the continuum domain, the NS solver determines the interface continuum fluxes by using the NS variables and DSMC-IP cell macroscopic information. Since the macroscopic information in the DSMC-IP cells is known in each time step, the DSMC-IP cells adjacent to the domain interface are treated as the ghost cells that provide the boundary conditions for flux computations.

Numerical Examples

Blunted Cone Tip

The first example is a 25° half angle cone with a blunted nose of 6.35 mm (0.25") in radius. The symmetric line of the cone is aligned with the free-stream. Only the upper half of the flow is considered, therefore. Since the wake region behind the cone is not of interest in this investigation, we assume that the cone is infinitely long but only the first 5 cm from the leading edge is considered. A structured grid, 600 cells along the body by 200 cells normal to the body, used in all computations is shown in Fig. 2.

The fluid is pure nitrogen and the free-stream conditions are listed in Table 1. The mean-free-path in the free-stream is about 1.3×10^{-4} m, accordingly. These specific free-stream conditions correspond to the Run 31 of CUBRC experiments.[20]

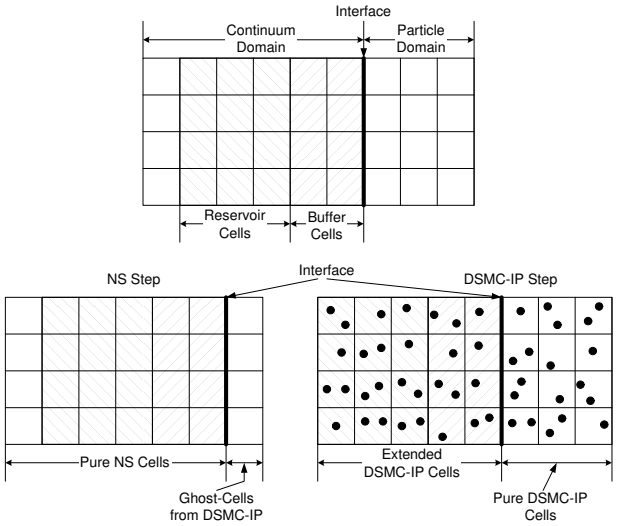

Fig. 1 Interface cell types.

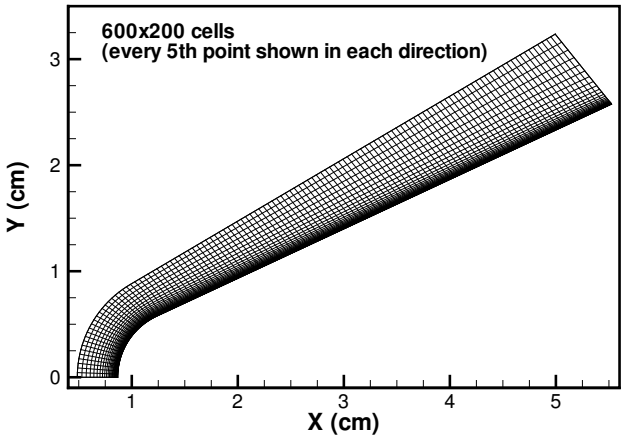

Fig. 2 Grid employed for 25° blunted cone.

In the CFD calculation, $\mu_{\text{ref}} = 1.656 \times 10^5$ N·s/m^2, $T_{\text{ref}} = 273$ K and $\omega = 0.74$. The Prandtl number is considered as a constant of 0.72. An isothermal wall at a temperature of 297.2 K and an accommodation coefficient of unity are assumed.

Table 1 Free-stream conditions of the blunted cone numerical experiment.

U_∞ (m/s)	T_∞ (K)	ρ_∞ (kg/m^3)	M_∞
2764.5	144.4	5.113×10^{-4}	11.3

A pure DSMC steady state solution is obtained with the use of more than 4.3 million simulation particles at the end of the computation. The reference time step in the pure DSMC calculation is 2 nsec. 100,000 time steps of computation are performed and the last 20,000 time steps are sampled to obtain the results.

In the hybrid simulation, a steady state solution is first obtained by computing the entire flow field with an implicit CFD scheme. Using the steady state solution and Kn_{max}, locations of the interfaces between the continuum and the particle domains are deter-

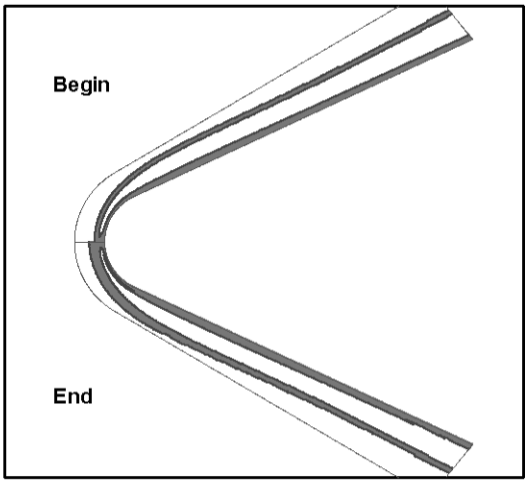

Fig. 3 Particle domain in hybrid simulation for a blunted cone.

mined. In the particle region, cell values are set to the CFD steady state results and simulation particles are initialized to the local Chapman-Enskog distribution.

Although it has been concluded in the previous work[12] that $\mathrm{Kn}_{\max} = 0.05$ is a good criterion for separating the two domains, a more conservative criterion of $\mathrm{Kn}_{\max} = 0.03$ is actually employed in this investigation. The particle domains initially and after 600,000 hybrid simulation iterations are illustrated in the shaded areas of Fig. 3. At beginning of the hybrid simulation, about 70.3% of the total number of cells are in the particle domain. This value increases gradually with time and reaches about 72.7% at the end of the simulation. Each cell in the particle domain has about 40 simulation particles on average. The reference time step in the hybrid computation is 0.2 nsec. The hybrid method results presented in this paper are obtained by sampling over the last 20,000 time steps.

The total run times of pure CFD, pure DSMC and hybrid codes on a Linux cluster with 1 GHz Intel® Pentium® III processors are: (1) approximately 2 hours on 10 processors for pure CFD; (2) approximately 30 hours on 10 processors for pure DSMC (MONACO); and (3) approximately 145 hours on 20 processors for the hybrid DSMC-CFD code.

Flow Fields

Comparisons of the translational temperature and density contours obtained with pure DSMC and the hybrid methods are made in Fig. 4. It it easy to observe in Fig. 4(a) that the bow shock thickness in front of the leading edge of the cone is thicker in the DSMC solution. Otherwise, the hybrid method results are in general in good agreement with the pure DSMC results. Additionally, the hybrid method provides much smoother results.

The hybrid results in Fig. 4 comprise two kinds of information. In the particle domains (the shaded area

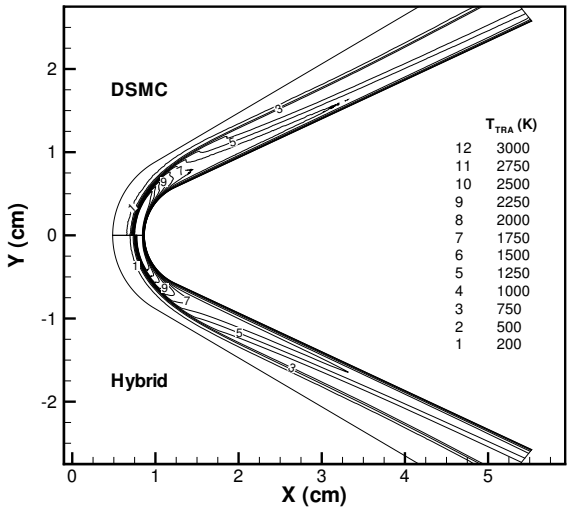

a) Comparison of translational temperature.

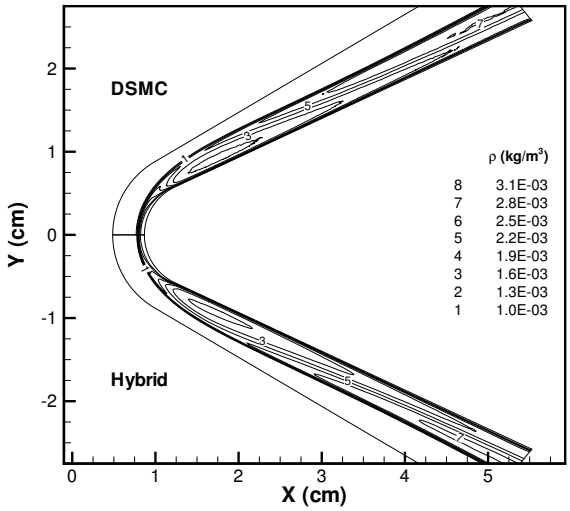

b) Comparison of mass density.

Fig. 4 Comparison of DSMC and hybrid solutions of translational temperature and mass density.

in Fig. 3) hybrid results are represented by IP information and in the continuum domains by NS information.

Surface Properties

In Fig. 5, comparisons of flow properties along the cone surface are made. The pressure coefficient and Stanton number in Fig. 5 are defined as

$$C_p = \frac{p - p_\infty}{\frac{1}{2}\rho_\infty U_\infty^2}, \qquad St = \frac{q_w}{\frac{1}{2}\rho_\infty U_\infty^3}.$$

In these figures, the profiles with label "Hybrid (DSMC)" represent only the DSMC information and with label "Hybrid (IP)" only the the IP information. Generally speaking, the flow properties predicted by the hybrid method along the wall are just in qualitative agreement with the DSMC solutions. This is because of the strong bow shock ahead of the cone tip and the IP method is not expected to work well under

such a nonequilibrium condition.[21] As a result, the entire downstream region is affected by the flow from the tip.

Detailed Comparisons

In Fig. 6, the pure DSMC, CFD and hybrid solutions are compared in detail along the stagnation line. The horizontal dotted lines in the figures indicate the interfaces between the continuum (upper) and particle (lower) domains. Similar to the contour plots above, the profiles labeled with "Hybrid (IP/NS)" consist of two kinds of information which are IP information in the particle domain and NS information in the continuum domain. The profiles with label "Hybrid (DSMC)" contain only the DSMC information in the particle domain and no information in the continuum domain.

Flow along this stagnation line can be viewed as a hypersonic flow that passes through a strong normal shock and rapidly decelerates to rest at the wall. In the shock wave, the flow is strongly nonequilibrium, and the CFD, IP and pure DSMC solutions are therefore expected to be different to a large extent. In Fig. 6(a), it is evident that the shock thickness and strength represented by the hybrid-IP/NS result are significantly different from the DSMC result. This is consistent with what is shown in Fig. 4(a). On the other hand, the hybrid-DSMC results are in good agreement with the pure DSMC results and prove that the hybrid technique really improves the physical accuracy compared to CFD.

A similar comparison between the pure DSMC, CFD and hybrid solutions for translational temperature, density and velocity at $x = 2$ cm is displayed in Fig. 7. At this location, the nonequilibrium effects start to weaken, and the Navier-Stokes equations coupled with a slip-boundary model perform fairly well. As shown in the figures, the CFD and DSMC solutions are close except in the shock region.

The whole computational domain at this location is divided into four sub-domains along the δn direction: particle (I: $0 < \delta n < 1$), continuum (II: $1 < \delta n < 3$), particle (III: $3 < \delta n < 3.95$) and continuum (IV: $\delta n > 3.95$). It is shown in Figs. 7(a) and 7(b) that the temperature and density predicted by the hybrid approach are in fair agreement with the pure DSMC solutions, except near the shock region. The velocity profile in Fig. 7(c) exhibits unexpected behavior at the interface between regions I and II. A similar behavior was also observed in the previous numerical experiment[13] and was concluded to be probably due to the size of region III being too small.

The whole computational domain is also divided into four sub-domains along the δn direction at $x = 4$ cm. Comparisons of translational temperature, density and velocity profiles obtained with the different methods are plotted in Fig. 8. In general, the results

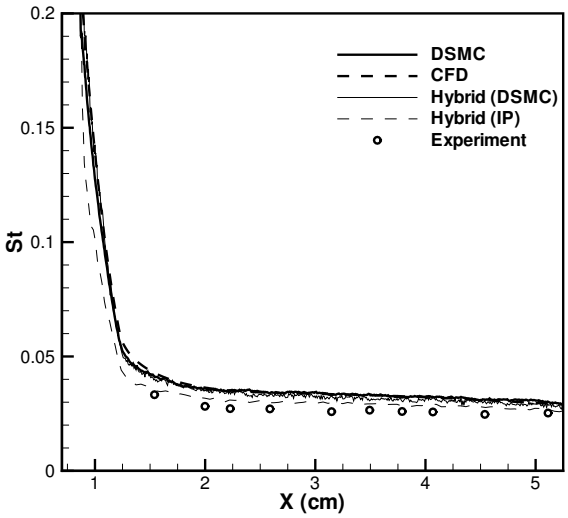

a) Comparison of surface heat transfer rate.

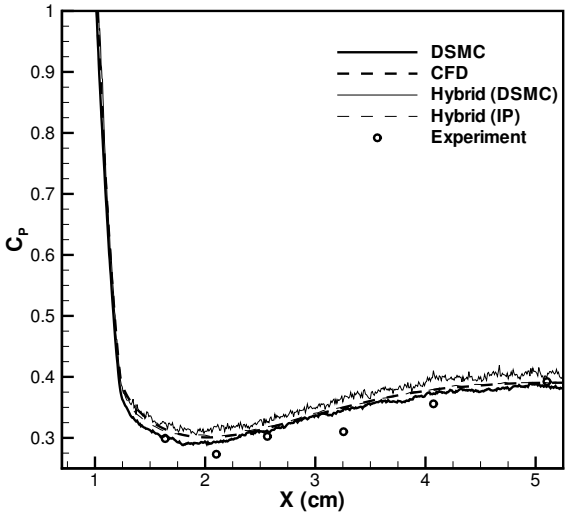

b) Comparison of surface pressure.

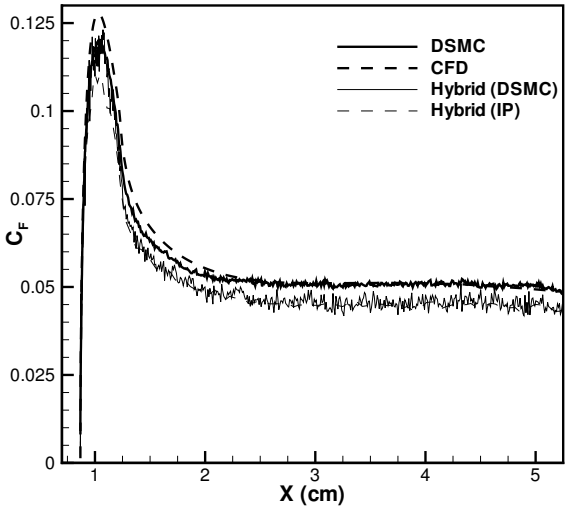

c) Comparison of skin friction coefficient.

Fig. 5 Comparison of surface properties with different numerical approaches.

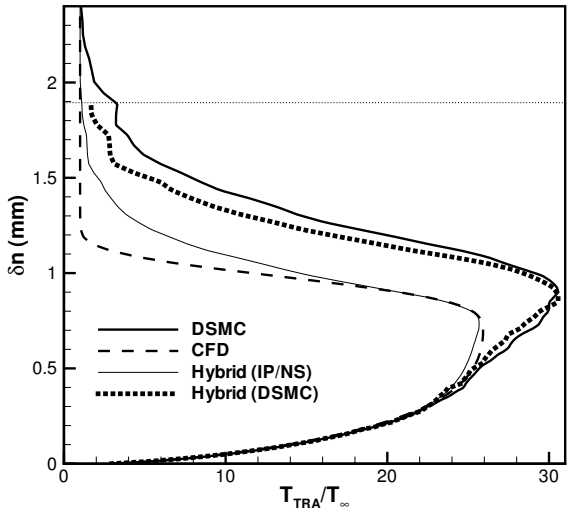

a) Comparison of temperature.

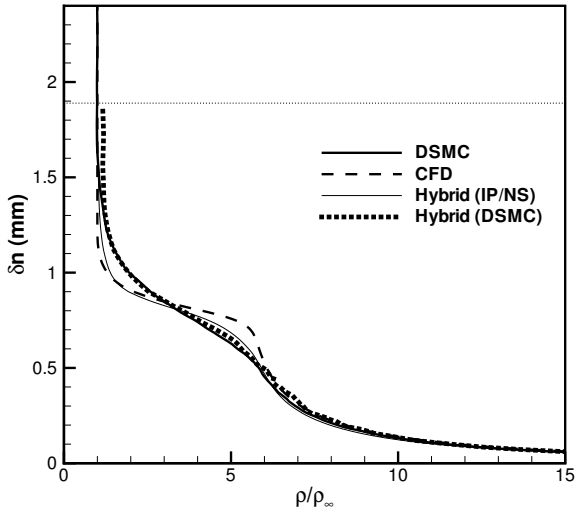

b) Comparison of temperature and density.

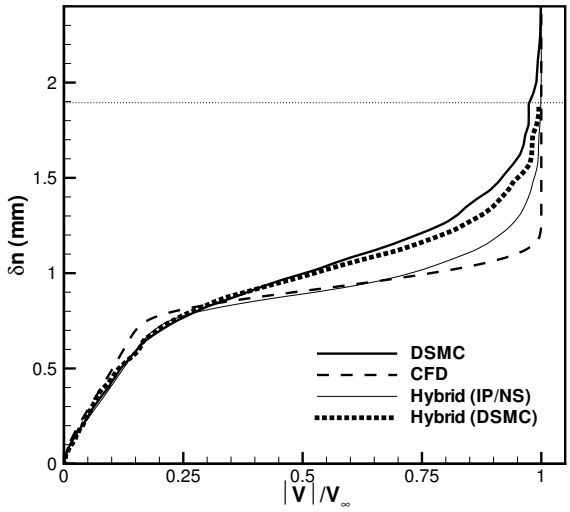

c) Comparison of velocity.

Fig. 6 Profiles along the line normal to the stagnation point.

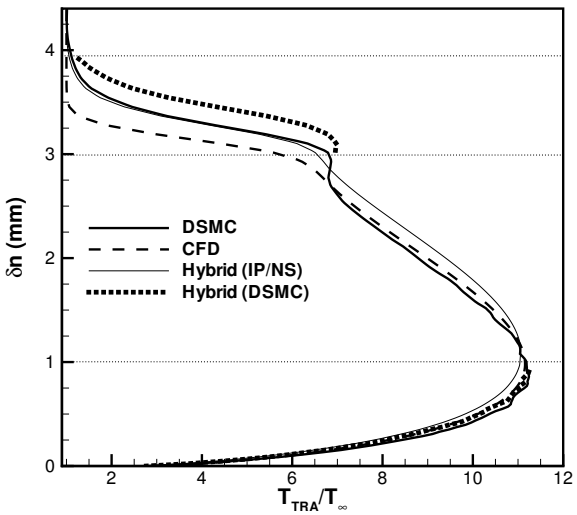

a) Comparison of temperature.

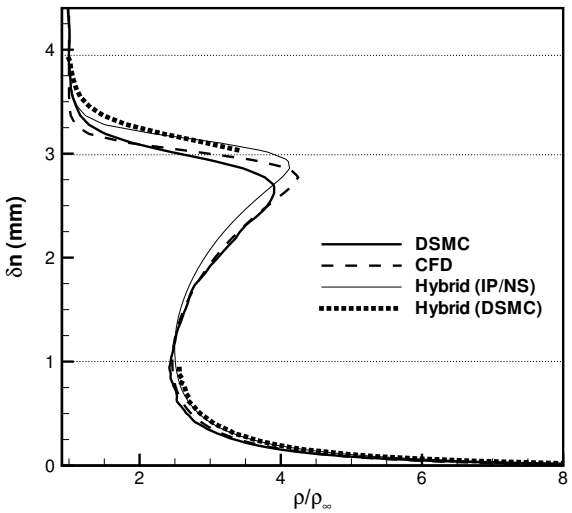

b) Comparison of temperature and density.

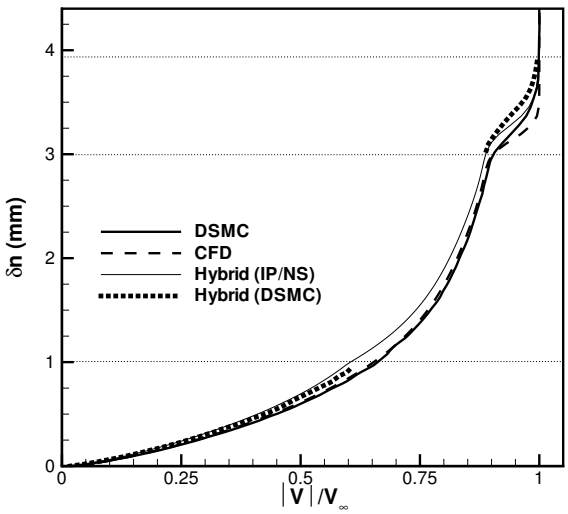

c) Comparison of velocity.

Fig. 7 Profiles along the line normal to the cone at x = 2 cm.

calculated by using the hybrid approach qualitatively agree with the pure DSMC results and have the same problems as in Fig. 7.

There is another problem associated with the hybrid-DSMC temperature on the interface between sub-domain III and IV in Fig. 8(a). The hybrid-DSMC temperature is higher than the pure DSMC temperature by a factor of 2 on the interface but the hybrid-IP/NS temperature looks very close to the pure DSMC temperature. This significant difference implies that the velocity distribution for particles entering from the continuum domain into the particle domain is not approximated by the IP temperature. This behavior is not yet understood and requires further study.

Hollow Cylinder-Flare

The configuration of the next example consists of a hollow cylinder followed by a 30° conical flare, as depicted in Fig. 9. The cylinder is aligned with the free stream. The leading edge is sharp and the hypersonic flow entering the hollow body does not interact with the external flow. Only the external flow of the upper half of the configuration is of interest in this example.

The fluid is also pure nitrogen and the freestream conditions are listed in Table 2. Notice that the freestream is nonequilibrium as the translational and vibrational temperatures are not the same. These are the nonequilibrium freestream conditions in CUBRC Run 14.[22] Since the IP method at this point is not capable of handling this type of nonequilibrium condition, the vibrational temperature is assumed to be frozen in all simulations. This means that the newly generated particles are initialized with the freestream vibrational temperature and all particles undergo no vibrational energy exchange for collisions with the wall which is assumed to be at a constant temperature of 295.6 K. The accommodation coefficient for translation energy is still assumed to be unity.

Table 2 Freestream conditions of the hollow cylinder-flare numerical experiment.

U_∞ (m/s)	T_∞ (K)	$T_{vib,\infty}$ (K)	ρ_∞ (kg/m^3)	M_∞
2301.7	118.2	2497.4	9.023×10^{-4}	10.4

The DSMC and hybrid codes are run on a structured grid that has 200,000 cells, with 1,000 cells along the body surface and 200 cells normal to the body surface, as shown in Fig. 10. A much finer grid that has 2048 cells along the surface and 512 cells normal to the surface is employed in the pure CFD simulation.[23] The hybrid code is initialized with the pure CFD steady state solution by interpolation.

A pure DSMC steady state solution is obtained with the use of more than 7 million particles at the end of the computation. The reference timestep is 3.5×10^{-9} sec. A total of 900,000 time steps of computation are

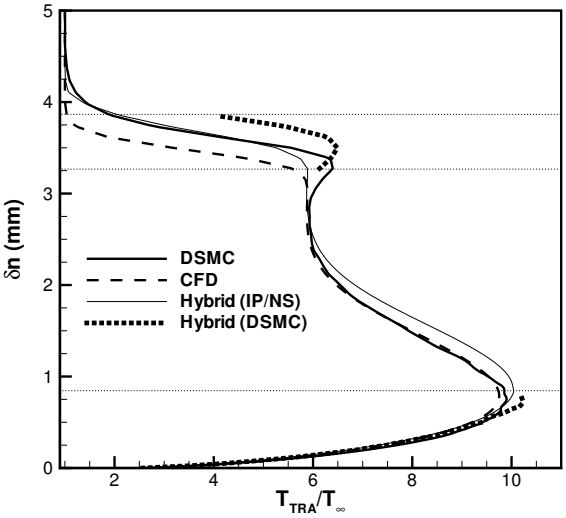

a) Comparison of temperature.

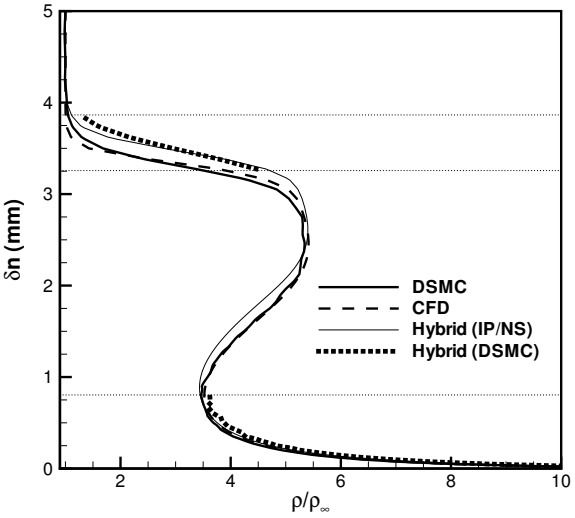

b) Comparison of temperature and density.

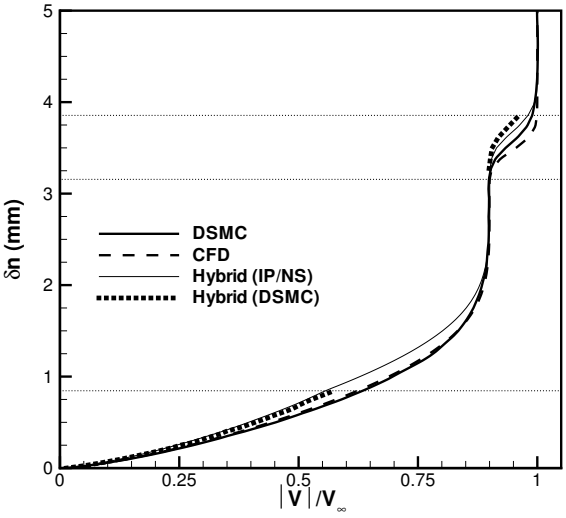

c) Comparison of velocity.

Fig. 8 Profiles along the line normal to the cone at x = 4 cm.

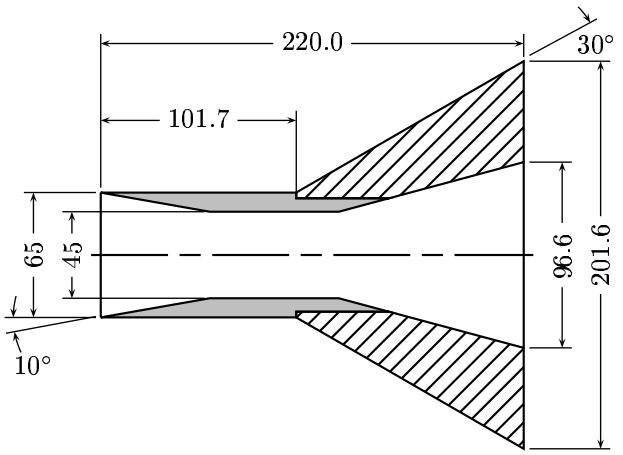

Fig. 9 Schematic of the CUBRC hollow cylinder-flare configuration (measurements in mm).

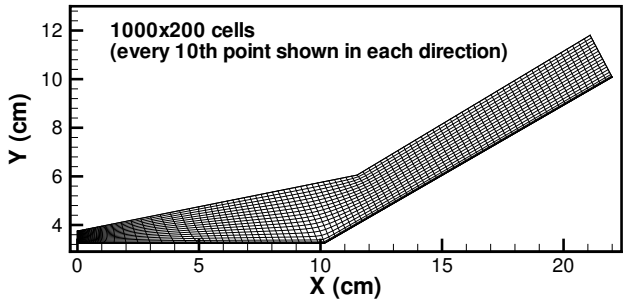

Fig. 10 Grid employed for hollow cylinder-flare.

completed and the last 20,000 time steps are sampled to obtain the results.

In the hybrid calculation, $\mathrm{Kn}_{\max} = 0.03$ is again employed as the breakdown criterion. The time step is 10^{-10} sec. A total of one million steps are computed after the domain is initialized with the CFD solution and the last 100,000 steps are sampled. At the beginning of the hybrid simulation, about 32% of the total number of cells are in the particle domain and at the end of the simulation, about 33% are in the particle domain. Since the particle domain undergoes just minor change during the simulation, only the final distribution is shown as the gray region in Fig. 11. Notice that a large portion of the particle domain is above the cylinder, where low density is encountered. The other portion of the particle domain is primarily along the shock waves and the body surface. Notice that there is a large continuum domain near the conjunction of cylinder and flare. There are about 40 particles in each particle cell.

The total run times of pure DSMC and hybrid DSMC-CFD codes on a Linux cluster with 2.4 GHz Intel® Xeon™ processors are: (1) approximately 82 hours on 20 processors for pure DSMC (MONACO); and (2) approximately 85 hours on 20 processors for the hybrid DSMC-CFD code.

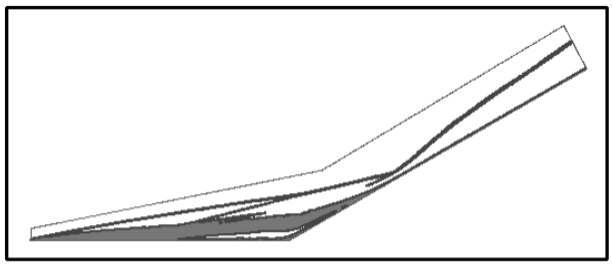

Fig. 11 Particle domain in hybrid simulation for a hollow cylinder-flare.

Flow Fields

Comparisons of the translational temperature and density contours obtained with pure DSMC and the hybrid method are shown in Fig. 12. It is very encouraging that the two solutions are in fair agreement under such complex circumstance.

Surface Properties

In Figs. 13(a) and 13(b), numerical results are compared with the experimental data[‡] from Ref. 22 for heat transfer rate and pressure coefficient along the body surface. Notice that there is about a 4% difference for the freestream density between the numerical simulations and the experiment. In general, the hybrid-DSMC and hybrid-IP results are in good agreement with the measured data. The Stanton number in Fig. 13(a) shows that the size of the separation and re-attachment region is under-predicted by DSMC but over-predicted by CFD. The pressure coefficient in Fig. 13(b) also indicates that DSMC in fact under-predicts the separation zone. This raises the question of whether DSMC really provides a physically accurate solution for this type of flow after the separation point at about $x/L = 0.5$ (L is the cylinder length and is 10.17 cm). The answer to this question is probably negative. Nonetheless, it is reasonable to assume that DSMC does provide the correct solution before the separation point. Skin friction coefficients calculated with different numerical methods are compared in Fig. 13(c). It is also clear that the size of the separation zone predicted by DSMC is different from CFD.

Detailed Comparisons

Detailed comparisons of the pure DSMC, CFD and hybrid solutions are first made along the line normal to the cylinder surface at $x/L = 0.01$, as displayed in Fig. 14. The comparisons all show that the hybrid-DSMC results are in outstanding agreement with the

[‡]The actual freestream conditions in experiment are: $U_\infty = 2325.6$ ms/s, $\rho_\infty = 8.658 \times 10^4$ kg/m^3, $T_\infty = 120$ K and $T_{vib,\infty} = 2287.2$ K.

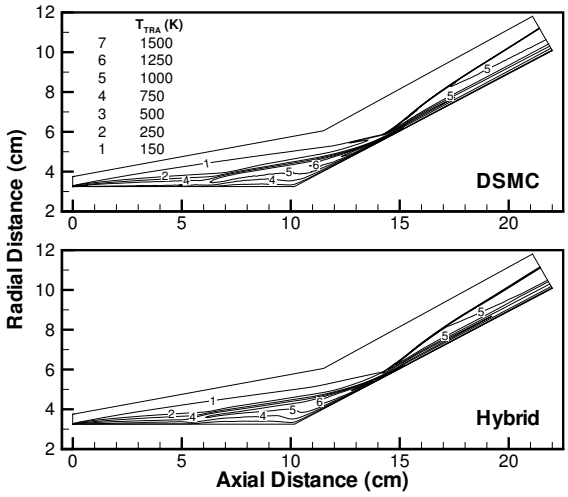

a) Comparison of translational temperature.

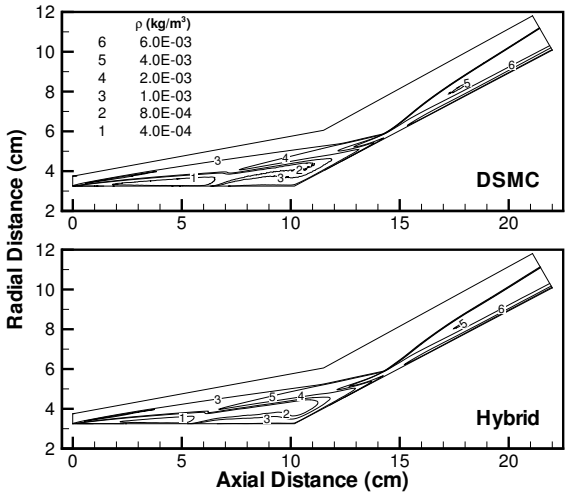

b) Comparison of mass density.

Fig. 12 Comparison of DSMC and hybrid solutions of translational temperature and mass density.

pure DSMC results.

Next, the flow field around the middle of the cylinder is studied. In Fig. 15, profiles are shown of comparisons for the flow properties along the line normal to the cylinder body at $x/L = 0.5$. At this station, the whole computational domain is divided into four sub-domains along the δn direction and hybrid-DSMC information is absent in a continuum domain. As mentioned above, it is reasonable to assume at this station that the pure DSMC solution is correct. In the particle domain next to the body, the hybrid-DSMC results again are predicted excellently by the hybrid DSMC-CFD code. The density profiles in Fig. 15(b) indicate that the density is as low as 30-40% of the freestream density at about $\delta n = 2$ mm. This can also be observed in Fig. 12(b).

In the shock region, both hybrid IP and hybrid DSMC results are only in qualitative agreement with

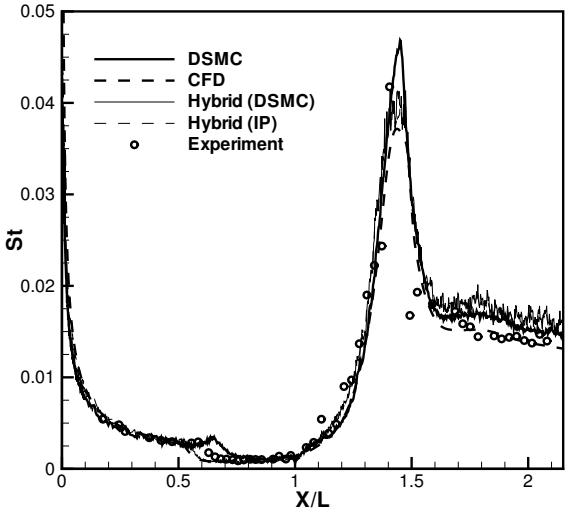

a) Comparison of surface heat transfer rate.

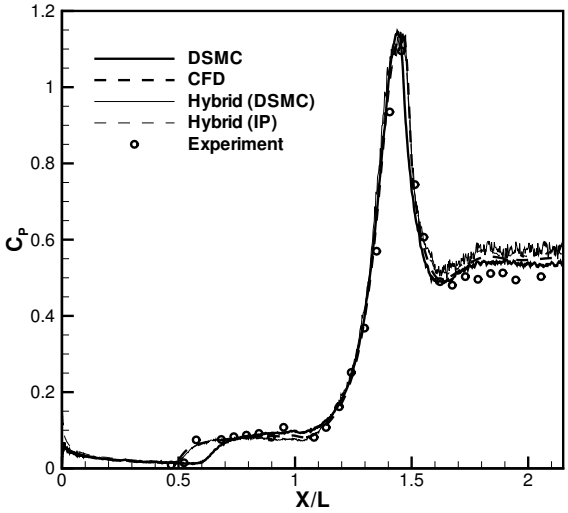

b) Comparison of surface pressure.

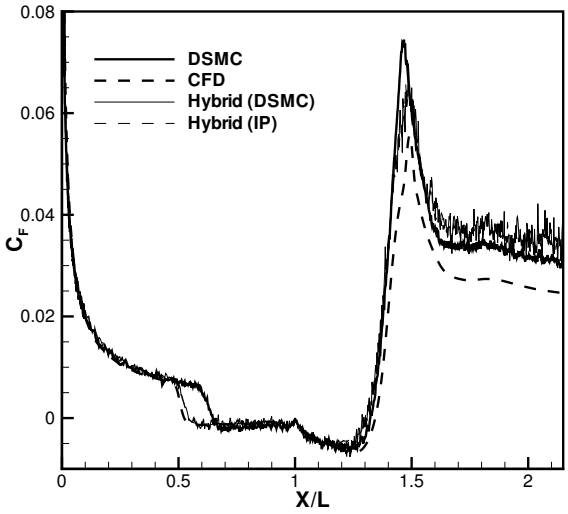

c) Comparison of skin friction coefficient.

Fig. 13 Comparison of surface properties with different numerical methods and experiment data.

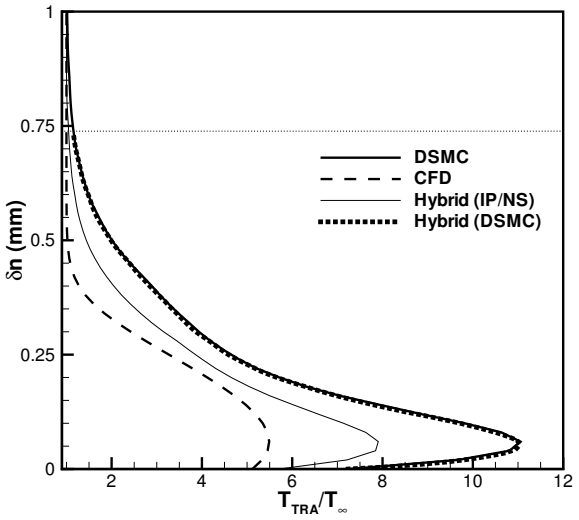

a) Comparison of temperature.

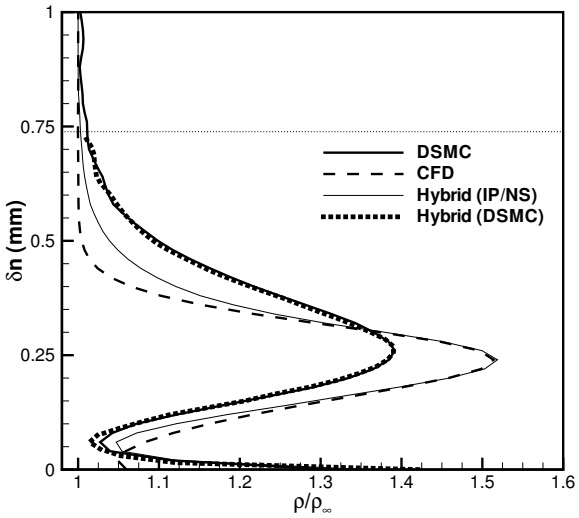

b) Comparison of temperature and density.

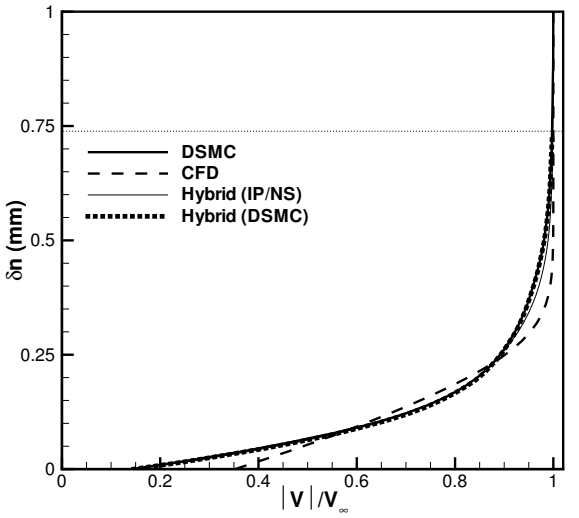

c) Comparison of velocity.

Fig. 14 Profiles along the line normal to the cylinder at x/L = 0.01.

DSMC, but at least they move from the initial CFD conditions towards the DSMC solutions.

Further downstream at the conjunction of the cylinder and flare ($x/L = 1$), profiles along a vertical line are shown in Fig. 16. The whole computational domain consists of six sub-domains along the δn direction. Since the accuracy of the pure DSMC solution at this station is questionable, it is difficult to judge the performance of the hybrid code. In most cases, the hybrid-IP/NS and hybrid-DSMC results stay with the initial CFD conditions, as shown in Figs. 16(a) and 16(b). Notice that the small discontinuity predicted by pure DSMC around the shock region is not predicted by any other methods.

Finally, a station on the flare is examined. Flow profiles along the line normal to the flare at $x/L = 1.3$ are plotted in Fig. 17. It is evident in Fig 17(b) that the discrepancy of the oblique shock angles predicted by pure DSMC and pure CFD is substantial. The hybrid code continues to remain closer to the CFD result.

It is interesting to point out that the hybrid-DSMC temperature in shock regions basically follows the corresponding hybrid-IP/NS temperature at all stations considered and the strange behavior in Fig. 8(a) is not observed in this example. This is possibly because the oblique shock wave in this example is weaker than the bow shock in the blunted cone flow.

Summary and Conclusions

The main objective for developing a hybrid particle-continuum method is a faster and more accurate approach than other conventional means. We have described such a method for computing hypersonic, nonequilibrium flows in 2D/axi-symmetric configurations. In the particle domain, the DSMC-IP technique was employed while in the continuum domain, a finite volume, second-order accurate, Steger-Warming flux vector splitting NS solver was utilized. Since the macroscopic values of the flow field in the DSMC-IP approach are updated in cells for each time step advanced, coupling these two domain becomes straightforward. Information exchange on the interface between the particle and continuum domains was continuously carried out for each time step.

Numerical experiments of hypersonic flows over a blunted cone and a hollow cylinder-flare body were conducted, with the use of the continuum-breakdown criterion $\mathrm{Kn}_{\max} = 0.03$. The hybrid method was first initialized with a steady state CFD solution and then marched forward. It is concluded that the hybrid method is capable of simulating these hypersonic flows fairly well, generally speaking. The detailed comparisons showed that the flow properties (temperature, density and velocity) computed with the hybrid method matched with the exact (pure DSMC) solutions in the regions near the bodies faithfully, but

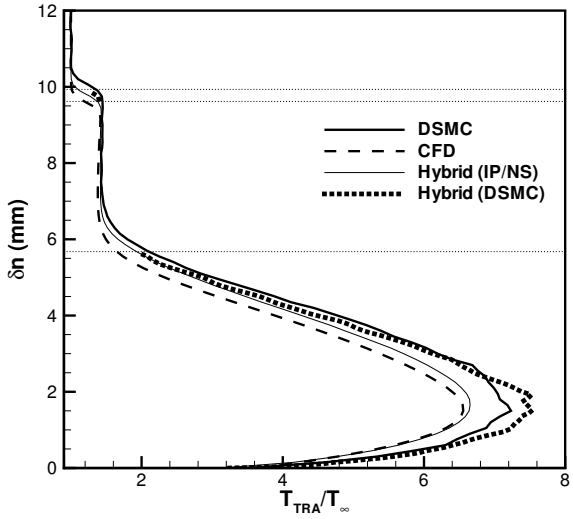

a) Comparison of temperature.

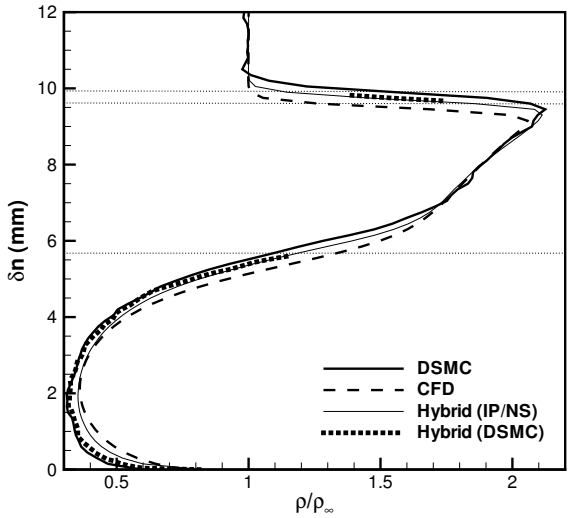

b) Comparison of temperature and density.

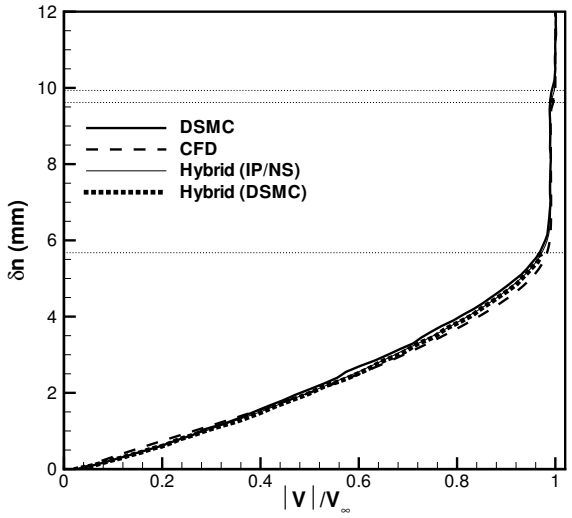

c) Comparison of velocity.

Fig. 15 Profiles along the line normal to the cylinder at x/L = 0.5.

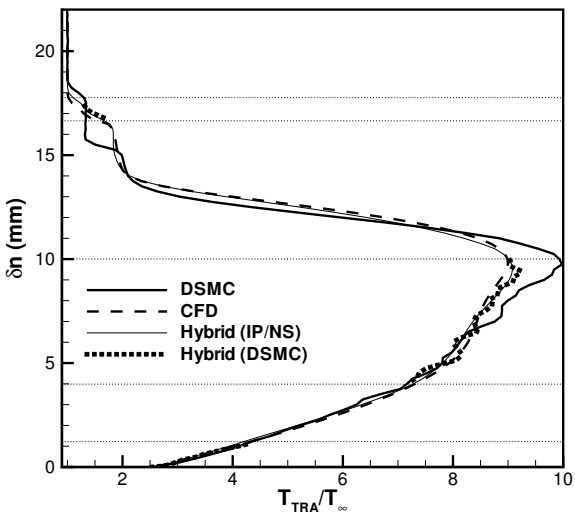

a) Comparison of temperature.

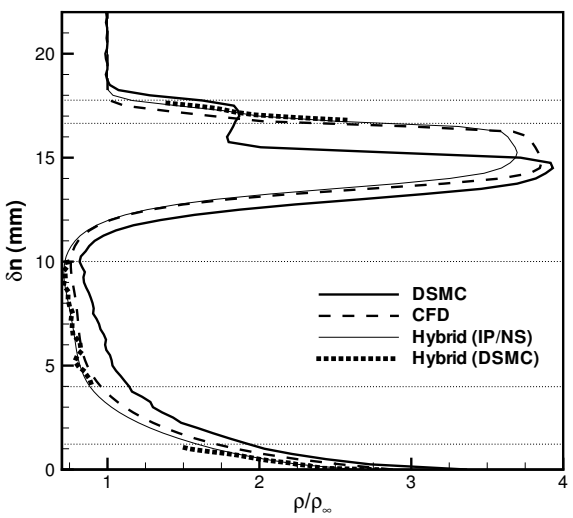

b) Comparison of temperature and density.

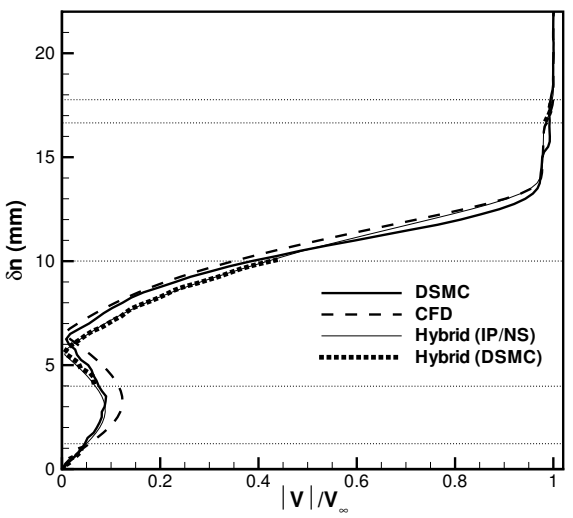

c) Comparison of velocity.

Fig. 16 Profiles along the line normal to the cylinder at x/L = 1.0.

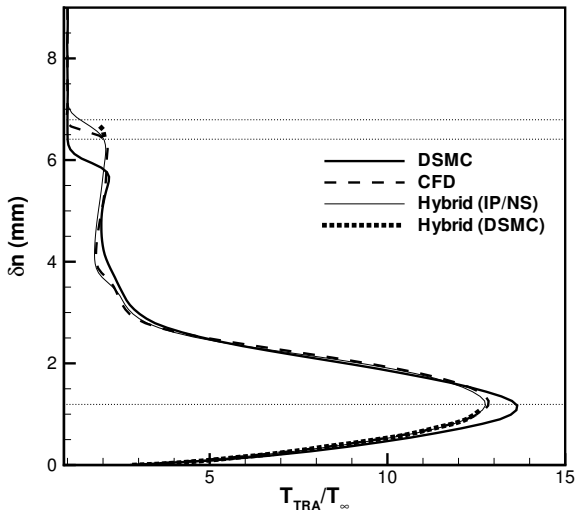

a) Comparison of temperature.

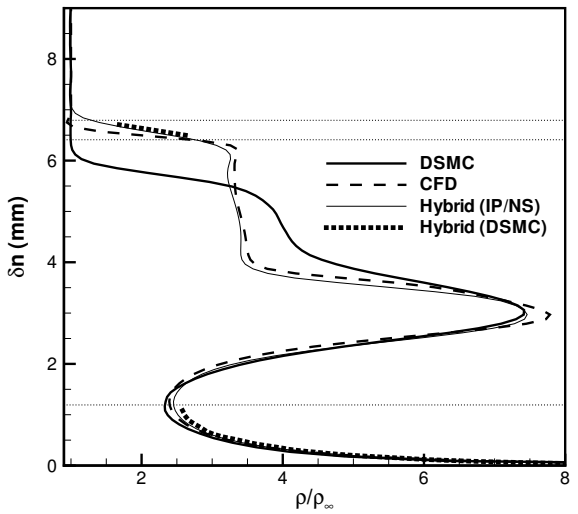

b) Comparison of temperature and density.

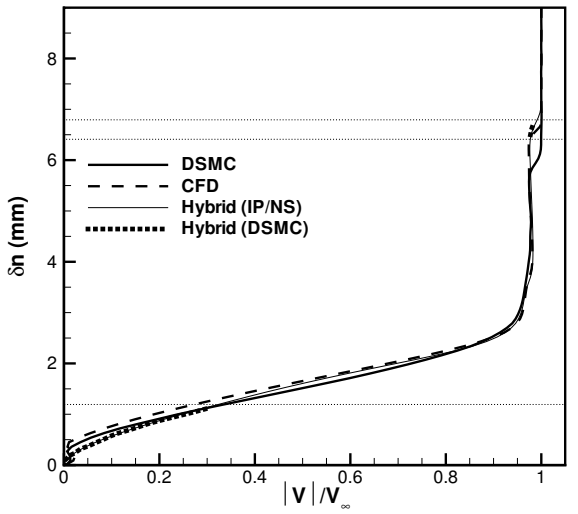

c) Comparison of velocity.

Fig. 17 Profiles along the line normal to the flare at x/L = 1.3.

poorly in shock regions.

The disappointing performance of the hybrid method in strong shock regions is primarily caused by the equilibrium assumption in the DSMC-IP technique to estimate the extra translational energy carried by a molecule moving from one cell to the other. A new energy flux model that can relax this assumption has been successfully developed[21] and will be integrated with the hybrid method in the near future.

The numerical efficiency of the current hybrid method also is a concern. The time step employed in a typical hybrid simulation is always an order of magnitude smaller than in the standard DSMC simulation because the DSMC-IP method requires such a small time step. In addition, the DSMC-IP method uses more memory than in the standard DSMC method. It is therefore concluded that the numerical efficiency of the hybrid method is far from satisfactory.

The level of physical modeling implemented so far in the hybrid code is only capable of simulating a perfect simple gas. As the purpose of developing a hybrid code is specifically intended for hypersonic flow with local regions of nonequilibrium, the level of physical modeling needs to be raised to include the ability to simulate thermal nonequilibrium of rotational and vibrational molecular modes, as well as finite-rate, nonequilibrium chemistry. For DSMC and CFD, methods for modeling the thermochemical nonequilibrium are available, but for the DSMC-IP method, schemes for modeling these same processes are yet to be developed.

Acknowledgments

The authors gratefully acknowledge Professor Graham Candler of University of Minnesota for providing the CFD code and Ioannis Nompelis for providing the CFD solution of the second example. The views and conclusions contained herein are those of the authors and should not be interpreted as necessarily representing the official policies or endorsements, either expressed or implied, of the AFOSR or the U.S. Government. The authors would also like to express thanks for the assistance from the University of Minnesota Department of Aerospace and Mechanics Computational Facilities.

This work was sponsored by the Air Force Office of Scientific Research under grant F49620-01-1-0003.

References

[1]Bird, G. A., *Molecular Gas Dynamics and the Direct Simulation of Gas Flows*, Oxford University Press, Oxford, 1994.

[2]Hash, D. B. and Hassan, H. A., "Assessment of Schemes for Coupling Monte Carlo and Navier-Stokes Solution Methods," *Journal of Thermophysics and Heat Transfer*, Vol. 10, No. 2, 1996, pp. 242–249.

[3]Chou, S. Y. and Baganoff, D., "Kinetic Flux-Vector Splitting for the Navier-Stokes Equations," *Journal of Computational Physics*, Vol. 130, No. 2, 1997, pp. 217–230.

[4]Lou, T., Dahlby, D. C., and Baganoff, D., "A Numberical Study Comparing Kinetic Flux-Vector Splitting for the

Navier-Stokes Equations with a Particle Method," *Journal of Computational Physics*, Vol. 145, No. 2, 1998, pp. 489–510.

[5]Garcia, A. L., Bell, J. B., Crutchfield, W. Y., and Alder, B. J., "Adaptive Mesh and Algorithm Refinement Using Direct Simulation Monte Carlo," *Journal of Computational Physics*, Vol. 154, No. 1, 1999, pp. 134–155.

[6]Rovedo, R., Goldstein, D. B., and Varghese, P. L., "Hybrid Euler/Particle Approach for Continuum/Rarefied Flows," *Journal of Spacecraft and Rockets*, Vol. 35, No. 3, 1998, pp. 258–265.

[7]Fan, J. and Shen, C., "Statistical Simulation of Low-Speed Unidirectional Flow in Transition Regime," *Proceedings of the 21th International Symposium on Rarefied Gas Dynamics, Marseille, France*, edited by e. a. R. Brum, 1998, p. 245.

[8]Fan, J. and Shen, C., "Statistical Simulation of Low-Speed Rarefied Gas Flows," *Journal of Computational Physics*, Vol. 167, No. 2, 2001, pp. 393–412.

[9]Cai, C., Boyd, I. D., Fan, J., and Candler, G. V., "Direct Simulation Methods for Low-Speed Microchannel Flows," *Journal of Thermophysics and Heat Transfer*, Vol. 14, No. 3, 2000, pp. 368–378.

[10]Sun, Q., Boyd, I. D., and Candler, G. V., "Numerical Simulation of Gas Flow Over Micro-Scale Airfoils," *Journal of Thermophysics and Heat Transfer*, Vol. 16, No. 2, 2002, pp. 171–179.

[11]Sun, Q. and Boyd, I. D., "A Direct Simulation Method for Subsonic, Micro-Scale Gas Flows," *Journal of Computational Physics*, Vol. 179, No. 2, 2002, pp. 400–425.

[12]Wang, W.-L. and Boyd, I. D., "Continuum Breakdown in Hypersonic Viscous Flows," AIAA Paper 2002–0651, Jan. 2002.

[13]Wang, W.-L., Sun, Q., and Boyd, I. D., "Assessment of a Hybrid Method for Hypersonic Flows," *Proceedings of the 23th International Symposium on Rarefied Gas Dynamics, Wistler, Canada*, edited by A. D. Ketsdever and E. P. Muntz, 2003, pp. 923–930.

[14]MacCormack, R. W. and Candler, G. V., "The Solution of the Navier-Stokes Equations Using Gauss-Seidel Line Relaxation," *Computers and Fluids*, Vol. 17, No. 1, 1989, pp. 135–150.

[15]Gökçen, T. and MacCormack, R. W., "Nonequilibrium Effects for Hypersonic Transitional Flows Using Continuum Approach," AIAA Paper 1989–0461, Jan. 1989.

[16]Sun, Q., *Information Preservation Methods for Modeling Micro-Scale Gas Flows*, Ph.D. thesis, Department of Aerospace Engineering, University of Michigan, 2003.

[17]Fan, J., Boyd, I. D., Cai, C.-P., Hennighausen, K., and Candler, G. V., "Computation of Rarefied Gas Flows Around a NACA 0012 Airfoil," *AIAA Journal*, Vol. 39, 2001, pp. 618–625.

[18]Dietrich, S. and Boyd, I. D., "Scalar and Parallel Optimized Implementation of the Direct Simulation Monte Carlo Method," *Journal of Computational Physics*, Vol. 126, 1996, pp. 328–342.

[19]Garcia, A. L. and Alder, B. J., "Generation of the Chapman-Enskog Distribution," *Journal of Computational Physics*, Vol. 140, No. 1, 1998, pp. 66–70.

[20]Holden, M. S., "Experimental Database from CUBRC Studies in Hypersonic Laminar and Turbulent Interacting Flows including Flowfield Chemistry," RTO Code Validation of DSMC and Navier-Stokes Code Validation Studies CUBRC Report, June 2000.

[21]Wang, W.-L. and Boyd, I. D., "A New Energy Flux Model in the DSMC-IP Method for Nonequilibrium Flows," AIAA Paper 2003–3774, June 2003.

[22]Holden, M. S., "Measurement in Regions of Laminar Shock Wave/Boundary Layer Interaction in Hypersonic Flow - Code Validation," CUBRC Report in CD-ROW, May 2003.

[23]Nompelis, I., private communication, April 2003.